SEARCH FOR HEAVY NEUTRINOS IN THE CAPTURE OF MUONS BY ^{3}He: DEVELOPMENT OF A HELIUM–FILLED GAS SCINTILLATION PROPORTIONAL COUNTER

B. Tasiaux, A.S. Carnoy, J. Deutsch, J. Egger, H. Kaspar, S. Lontie, C. Petitjean, R. Prieels and N. Rosier

Abstract

We have developed a high-pressure ^{3}He target based on the principle of a Gas Scintillation Proportional Counter (GSPC) to observe with high luminosity and good energy resolution tritons emitted in the capture of muons by ^{3}He. The techniques used with this new detector are described and the first results obtained in the search for massive neutrinos which couple to muons are shown.

1. Purpose

The ultimate goal of the experiment is to detect, with high sensitivity, a possible massive neutrino (with a mass between 20 MeV/c^2 and 90 MeV/c^2) admixed into the muon flavour. In the capture process of a negative muon by a ^{3}He nucleus a massive neutrino of this kind would manifest itself as an anomalous peak in the measured triton energy spectrum of the ^{3}H + ν_μ decay channel. The experiment required the development of a ^{3}He target which allowed the observation of the ^{3}H recoil spectrum with good resolution and background-rejection capacity.

2. Introduction

The neutrinos which couple to the charged leptons of various flavours could be superpositions of mass eigenstates of non-vanishing mass. The formulation of this scenario beyond the Standard Model (SM) is discussed in refs [1] and [2].

Most searches for lepton generation mixing have either been looking for ν oscillations or for ν decay of neutrinos emitted in nuclear reactors or accelerators. Cosmological observations form the other important source of information on this subject. Complementary information can also be obtained by studying the two-body decay of systems decaying into a charged particle and a neutrino [3]. In π^+ and K^+ decays [4–8] the energy spectrum of the emitted-charged muon was investigated. The contribution of a massive neutrino to ν_μ would manifest itself by the appearance of a peak with energy lower than the one corresponding to the $m_\nu = 0$ channel. The Q value limits this mass region to $m_\nu \leq 34$ MeV/c^2 ($\pi \rightarrow \mu + \nu$) and to $m_\nu \leq 388$ MeV/c^2 ($K \rightarrow \mu + \nu$) respectively. The experimental limitation of energy resolution which can be achieved limits moreover the covered mass region to $m_\nu \geq 1$ MeV/c^2, respectively $m_\nu \geq 70$ MeV/c^2.

We must keep in mind that the ν_3 mass is experimentally measured to be smaller than 35 MeV/c^2 [9], and that no massive neutrinos ν_i ($i > 3$) can be present below ~ 35 GeV/c^2 [10]. Moreover, neutrino masses larger than ~ 40 eV/c^2 are only compatible with astrophysical observations if the neutrinos are allowed to decay [11].

A system equivalent to the $\pi_{\mu 2}$ or $K_{\mu 2}$ processes is the one obtained if a μ is captured by a nucleus producing a two-body decay into a single nucleus–neutrino channel. Our experiment is of this type and measures the recoil energy spectrum of the triton (t) emitted after muon capture on ^{3}He.

The Q value of the reaction limits the range of the observable neutrino mass to the interval 20 MeV/c$^2 \leq m_\nu \leq 100$ MeV/c^2, which overlaps the sensitivity limits of the π_{e2} ($m_\nu \leq 30$ MeV/c^2) and K_{e2} ($m_\nu \geq 70$ MeV/c^2) experiments.

The presence of a peak of intensity $I(m_\nu)$ at a triton kinetic energy T_t would indicate the contribution to ν_μ of a neutrino of mass

$$m_\nu = \sqrt{\left(M_0 - M\left(^3H\right)\right)^2 - 2M_0 T_t} \ , \qquad (1)$$

where

$$M_0 = M\left(^3He\right) + m_\mu - E_{binding} \cong M\left(^3He\right) \ ,$$

$M(^3H)$, $M(^3He)$ and m_μ being the ^{3}H, ^{3}He and muon masses.

The ratio of $I(m_\nu)$ to the intensity of the ($m_\nu = 0$) peak gives the strength $U^2_{\mu i}$ of the coupling [12,13]

$$\frac{I(m_\nu)}{I(0)} = \frac{\Gamma(m_\nu)}{\Gamma(0)} = \frac{\rho(m_\nu)}{\rho(0)} U^2_{\mu i} \qquad (2)$$

with the phase space factor

$$\rho(m_\nu) = \left(\Delta^2 - m_\nu^2\right) \times \left[\left(1 - \frac{\Delta}{2M_0}\right)^2 - \left(\frac{m_\nu}{2M_0}\right)^2\right] , \qquad (3)$$

where $\Delta = M_0 - M(^3H) \cong m_\mu$.

3. Description of the detector

The apparatus is an active ^{3}He target (self-triggered TPC-like GSPC) specifically designed to measure the kinetic energy of the tritons produced in the capture of negative muons by ^{3}He. It is installed on the μE4 muon channel of the proton accelerator of the Paul Scherrer Institute (PSI).

© 1991 Gordon and Breach Science Publishers S.A.
Photocopying permitted by license only.

Particle World, Vol. 2, No. 3, p. 81–86, 1991.

Negative muons of 32 MeV/c momentum cross a telescope of two 0.5 mm thick scintillators and enter the detector through a 30 mg/cm^2 HAVAR (Hamilton Techn. Inc., Lancaster) window. They are stopped in the so-called stop region which is between a plate G_0 and a grid G_1 (fig. 1). The detector is filled with gas at a pressure of 5 bar; for an event considered as "good", the (μ ^{3}He) system decays into a triton and a muon-neutrino.

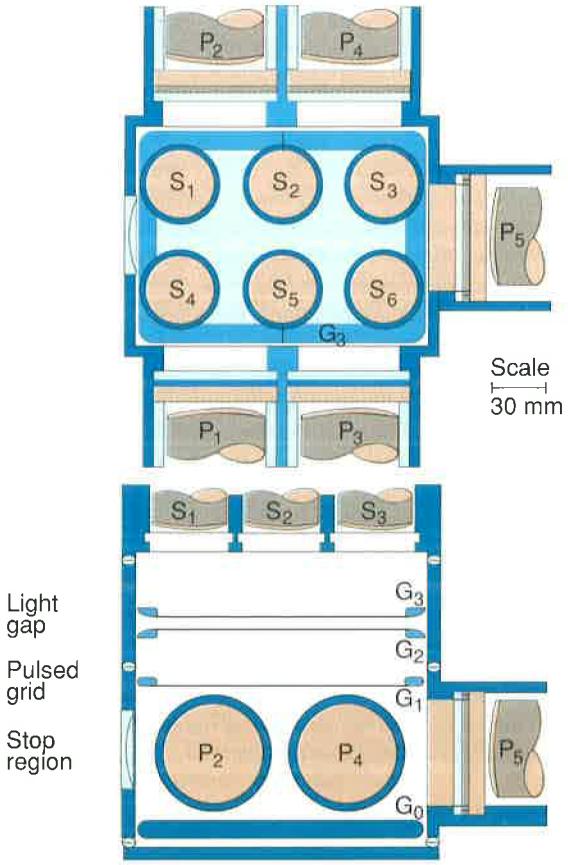

FIGURE 1

Horizontal and vertical projections of the GSPC indicating the G_0, G_1, G_2 and G_3 electrodes, the primary photomultipliers P_1 to P_5 and the secondary photomultipliers S_1 to S_6. The beam enters from the left in the G_0 to G_1 region.

Five single-photon photomultipliers EMI 9829QB (P_i) detect the primary scintillation light first produced by the stopping μ^- and then produced by the emitted triton; these two signals define, in coincidence with the muon signal from the two plastic scintillators of the telescope, a muon-captured event. The cloud of ionization electrons produced by the μ and t tracks is drifted in an electric field (300 V/cm, drift velocity $\approx$ 0.17 cm/μs) towards two grids G_2 and G_3, called light gap. The electric field in the light gap is so high (11 kV/cm) that the electrons excite the gas atoms thereby producing in successive electron–atom scatterings many thousands of scintillation photons per electron. The time-dependent behaviour of this "secondary" light, detected in six photomultipliers EMI 9903KB (S_i), is recorded in six wave-form analyzers (WFA) in 50 ns steps.

This information is used to reconstruct the position, track length, and energy of the muon and triton. In addition to this, full differential information, typical times (decay time, beginning and end time of the μ and t signals in the S_i photomultipliers) and integrated values of the μ and t signals for the primary and secondary light were recorded for a fast on-line analysis [14]. All these data were stored on magnetic tape for a given event if, and only if, a two-peak structure was observed on the sum of the S_i photomultiplier outputs.

In order to protect the five P_i photomultipliers from the large amount of light produced in the light gap, and to avoid spurious coincidences in waiting for the capture reaction after a muon stop, the high voltage on G_1 is set so as to collect on G_1 all the charges produced between G_0 and G_2. After a muon capture has occurred, the G_1 high voltage is pulsed for ~ 100 μs to a value allowing the relevant charge to drift into the light gap. During the same period, the five P_i photomultipliers are blanked by pulsing the photocathode voltage. This is done by applying a voltage pulse simultaneously to the photocathode and a grid mounted in front of it, in order to prevent the photoelectrons from reaching the first dynode.

In a second experiment, performed with the same detector, to be discussed on an other occasion, the gating function was realized by a supplementary grid installed just in front of G_2 with alternate wires pulsed to a voltage difference of 180 V. The protection of the P_i photomultipliers was performed in this second experiment by a suitable pulsing of their first dynodes.

The scintillation light of pure He (500–1000 Å) has to be shifted to the sensitivity region of the photomultipliers equipped with quartz windows ($\lambda \geq$ 1600 Å). This is done by mixing 10% of Xe to the ^{3}He target gas. With this mixture ~ 75% of the muons are captured on Xe and the detector has to be vetoed during the first 2 μs following the muon stop to allow most of the muons in atomic orbits on a Xe atom to be captured ($\tau \approx$ 100 ns). The stable and efficient running of the detector [15] compensates largely for this important loss (90%).

The detector is pressurized at 5 bar in order to have a stop density of a viable amount of muons in the fiducial volume ($7 \times 9 \times 13$ cm^3; $\approx$ 40 mg/cm^2). Under these conditions a high gas purity is necessary ($\leq$ 0.2 ppm of impurities) and high electric fields have to be applied. Special techniques, such as fixing the wires with a galvanic deposition of an Sn alloy on specially-shaped frames, had to be developed.

4. Analysis: construction of the recoil energy spectrum

The light in the gas, produced by the stopping muon and by the emitted-charged particle, the primary light, was detected by the

five P_i photomultipliers and gave timing information and the start signal for a potentially good triton decay sequence shown in fig. 2.

The energy spectrum was obtained from the light emitted in the light gap seen by the six S_i photomultipliers. The sharing of this light amongst the photomultipliers and the time structure of this light pulses allowed us to reconstruct the trajectory of the charged particles (i.e. muon and triton) and to identify the capture products.

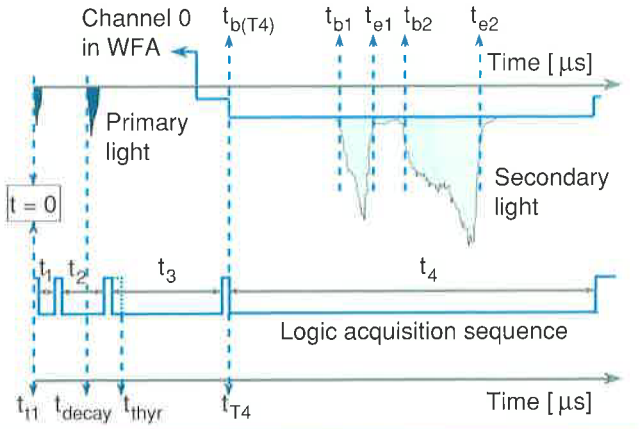

FIGURE 2

Pulse sequence of a good event: t_1 = time to let the μ^- Xe system disappear; t_2 = time interval to accept events from muon capture in ^{3}He; t_3 = time to adjust the drift field and the minimal drift time; t_4 = time to collect the secondary light from the muon and triton tracks.

The two peaks (muon, triton) separated by the time elapsed between the muon stop and the muon capture were obtained by synchronising the six photomultiplier amplitudes S_i (secondary light). Events that did not have this signal structure were rejected.

The gains of the S_i were adjusted by choosing a small region in the fiducial volume and observing the triton signals originating there. The drift velocities and diffusion coefficient required to reconstruct the muon–triton trajectories were determined by adjusting the parameters of the diffusion equation to fit the observed pulse shape.

The reconstruction of the initial trajectories and the determination of the energy deposition along these trajectories, as well as that of the total energies deposited, were performed in three steps:

(a) For each 50 ns sampling of the S_i amplitudes in which at least three were non-zero, a least-square adjustement allowed us to determine the intensity and the position of the corresponding flash in the light gap.

(b) In a second step, a linear fit was made to the positions of the flashes in the light gap as determined in the previous step. The flash position thus adjusted was considered as the "true" one and it served to re-determine the corresponding flash amplitude, which was assumed to be proportional to the energy deposited by the charged particles (muon, triton) in the stop region (G_0-G_1).

(c) The exact coordinates of these cells (cf. (a)) along the drift direction were determined using the drift velocity.

Due to field inhomogenities in the stop region, caused by the P_i photocathodes which were kept on ground potential, we observed variations in the drift velocity and position-dependent collecting efficiencies for the ionization electrons of the charged particles. These effects on the total amplitude were corrected for each event.

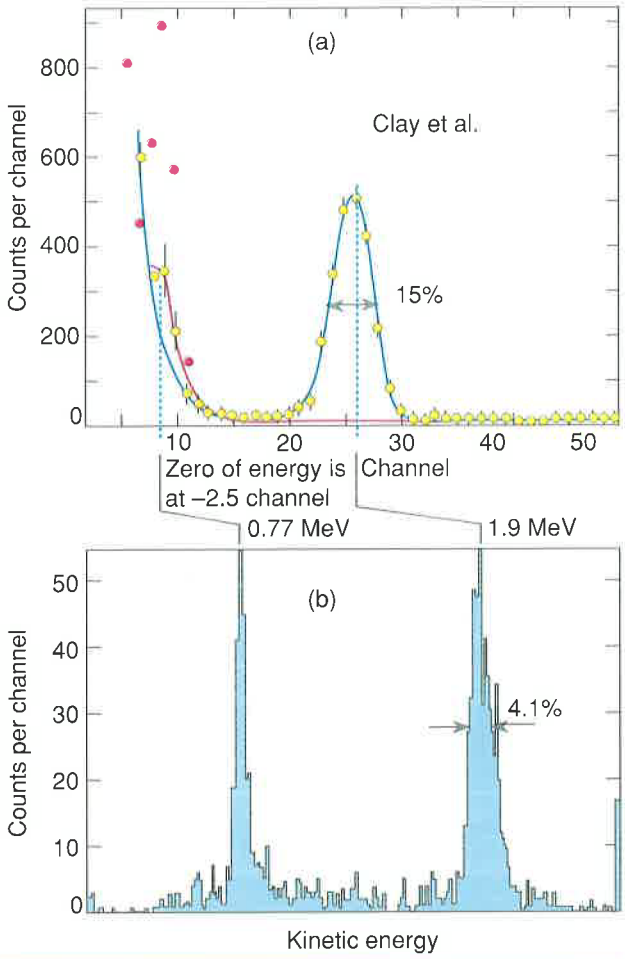

FIGURE 3

Comparison between the triton recoil energy spectrum obtained by Clay et al. [16] and the spectrum observed in this work.

The energy spectrum of the tritons, restricted to a small central region of the stop region has a FWHM resolution of 0.9%; if we consider a more extended fiducial volume of $6.5 \times 4.5 \times 3.0$ cm^3, we obtain the spectrum illustrated in fig. 3(b) in which the triton peak has a FWHM resolution of 4.1%.

In figs 3(a) and 3(b), we compare the obtained spectrum to the one observed by Clay et al. [16] using a conventional Gas Scintillation Detector (GSD) filled with ^{3}He. The improvement is due mainly to the localizing ability of our detector, which allows the rejection of energy deposition outside the fiducial volume and permits the correction of the variation of the solid angle in which the light is observed. Moreover, the enhanced light emission, in the light gap, decreases substantially the contribution of the statistical fluctuations. We learned that a careful shaping of the collecting electric field will allow us to improve the energy resolution to less than 1% FWHM as mentioned above [17].

5. Analysis: the background rejection

The energy spectrum of fig. 3 shows, in addition to the peak around 1.9 MeV, attributed to the tritons emitted in conjunction with a zero-mass neutrino, a peak around 0.77 MeV and a continous background. It is important to reject these various backgrounds if we wish to improve the sensitivity of the experiment.

The peak at ≈ 0.77 MeV is produced by accidental coincidences between a muon stop and the absorption of a neutron by ^{3}He nucleus

$$n + {}^3\mathrm{He} \rightarrow p + {}^3\mathrm{H} \qquad (Q = 0.774\ \mathrm{MeV})\ .$$

The remaining background is interpreted as originating from muon-decay electrons interacting in various materials and from protons or deuterons of the other capture channels:

$\mu^- + {}^3\mathrm{He} \rightarrow e^- + \nu_e + \nu_\mu + {}^3\mathrm{He}$	(99.47 %)	I
$\mu^- + {}^3\mathrm{He} \rightarrow \nu_\mu + {}^3\mathrm{H}$	(3.3×10^{-3})	II
$\mu^- + {}^3\mathrm{He} \rightarrow \nu_\mu + d + n$	(1.3×10^{-3})	III
$\mu^- + {}^3\mathrm{He} \rightarrow \nu_\mu + p + n + n$	(3.7×10^{-4})	IV

The integrated contribution of channels III and IV in the energy window of 0–2 MeV was calculated to be 1.5% and 6% respectively of the channel-II intensity, but protons and deuterons of higher energy losing only a part of their kinetic energy may also contribute to the background if no cut is applied on the length of their trace in the detector.

Various constraints were used to reject the background affecting only minimally triton recoils of 1.9 MeV or lower. Essentially, the procedure was the following:

(a) First we rejected the events in which the end of the first trajectory (muons) did not coincide with the beginning of the second trajectory (tritons), taking into account the drift distance before the emission of the triton. This cut rejected very effectively most of the accidental coincidences of the neutron capture peak at 0.77 MeV.

(b) Events with a distorted second track or showing no Bragg peak are rejected to ensure that the total charge was confined to the region of good charge collection.

(c) The biparametric range-energy plot of the second charged particle allowed us to define the region which should contain the recoil tritons; the events outside this region were also rejected.

(d) Finally, the shape of linear energy deposition along the trace can also be used to distinguish between triton and deuteron recoils (more difficult to reject by the range-energy constraint than the protons) as illustrated in figs 4 and 5.

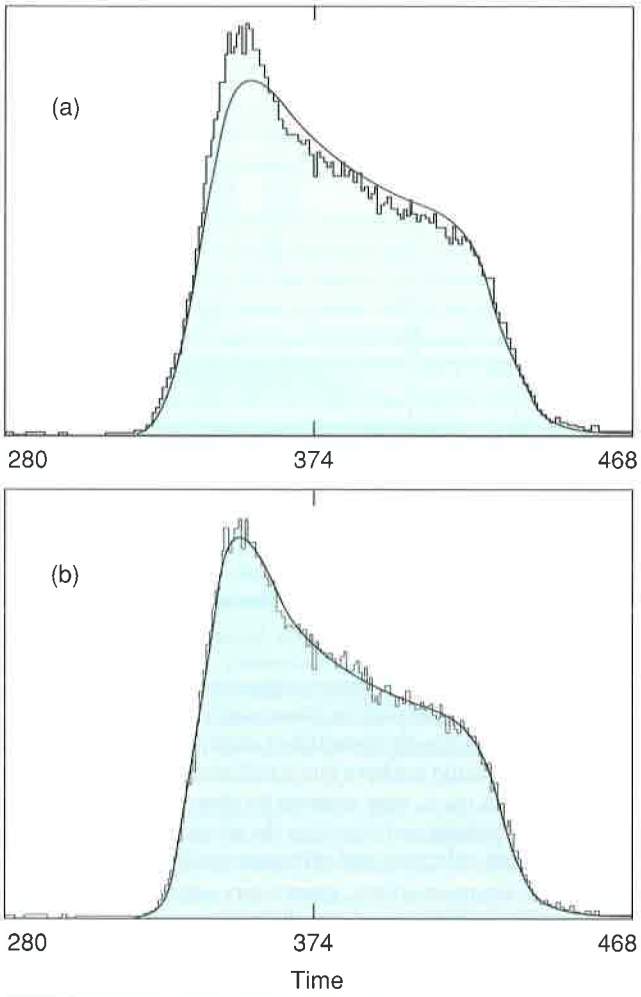

FIGURE 4

Deuteron event: (a) adjusted by a triton pulse and (b) adjusted by a deuteron pulse. Along the time axis, one bin represents 50 ns.

The effects of these various cuts are represented in fig. 6((a)–(e)).

The energy spectrum resulting from these cuts is represented in fig. 7. It is completely free of background at the limited statistical precision of this first part of the experiment. The number of 1.9 MeV triton recoils is 409, to be compared to 656 before the cuts were applied.

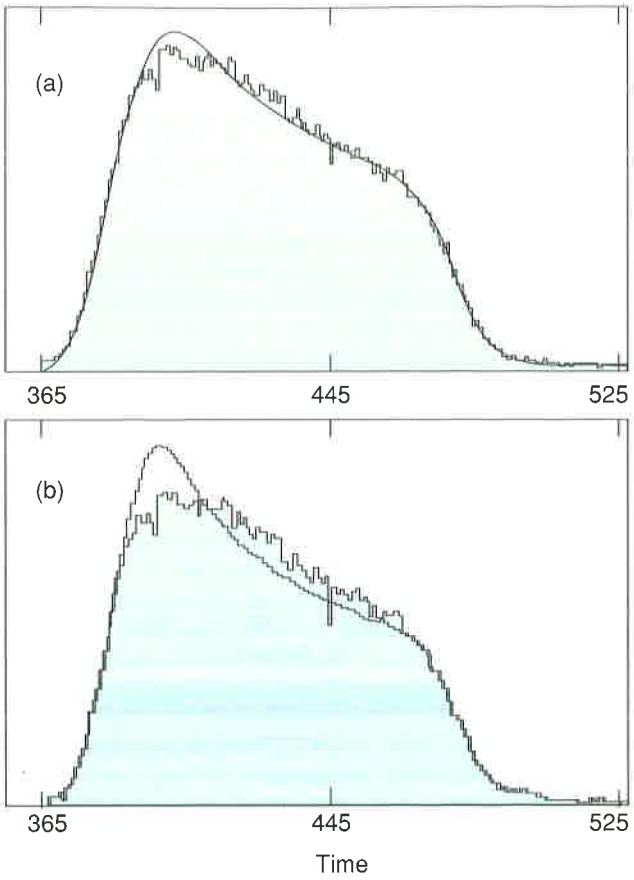

FIGURE 5

Triton event: (a) adjusted by a triton pulse and (b) adjusted by a deuteron pulse. Along the time axis, one bin represents 50 ns.

6. Conclusion

No massive neutrinos were found to contribute to the muon coupling; the corresponding 90% C.L. uppper limits are shown in fig. 8. Although the precision of these limits based on a small data sample is still moderate and, in particular, much worse than the ones deduced from the ($\pi \rightarrow \mu + \nu$) decay mode in the neutrino mass region of $m_\nu \leq 34$ MeV/c^2, the considerations discussed above allow to foresee a considerable improvement from the second experiment.

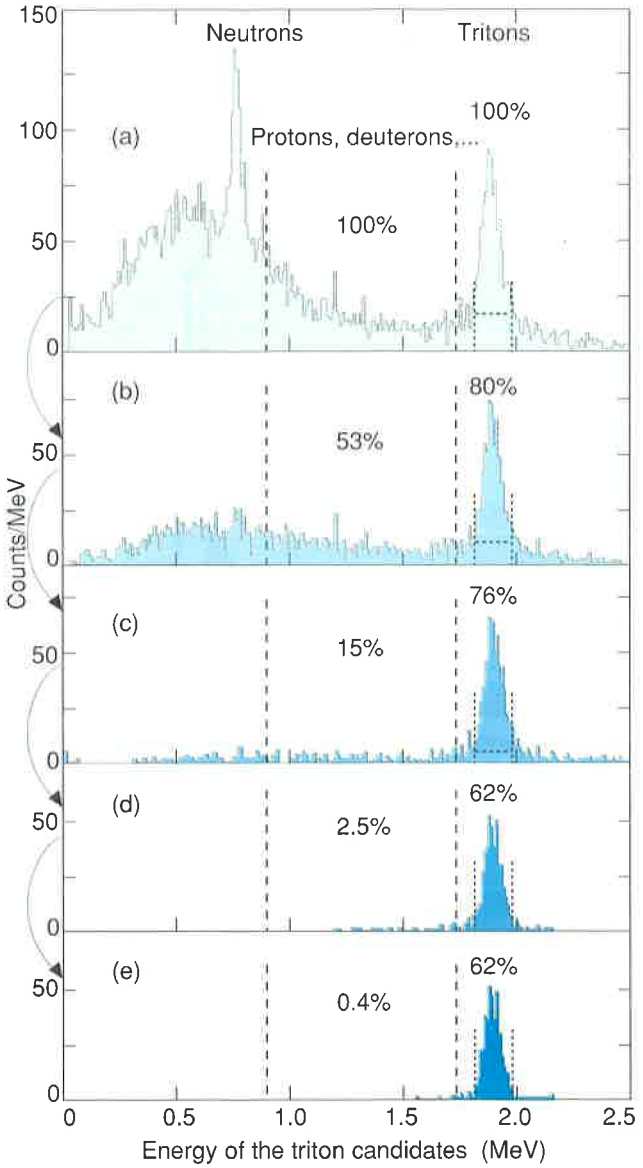

FIGURE 6

(a) initial spectrum; (b)-(e) spectra obtained after applying successively the four cuts discussed in the text. The numbers indicate the percentage of the background and of the signal which survive the cuts.

Acknowledgements

We thank G. Grégoire and T. Delbar for their participation in the early phases of the experiment and B. de Callatay, L. Meier and F. Pozar for their excellent technical support. The experiment benefitted from the competent work of many staff members from PSI and University of Louvain.

References

[1] F. Boehm and P. Vogel, Physics of massive neutrinos, Cambridge Univ. Press (1987).

[2] B. Kayser et al., The physics of massive neutrinos, World Scient. Lect., Notes in Phys., Vol. 25 (1989).

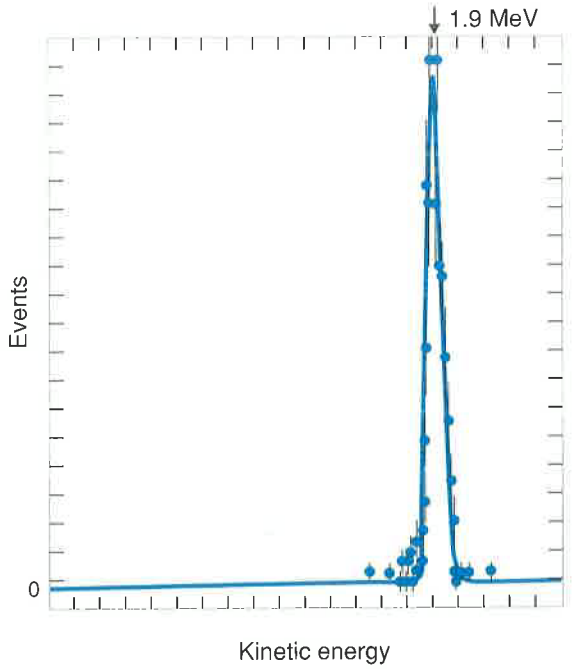

FIGURE 7

Triton recoil energy spectrum resulting from all cuts, completely free of background.

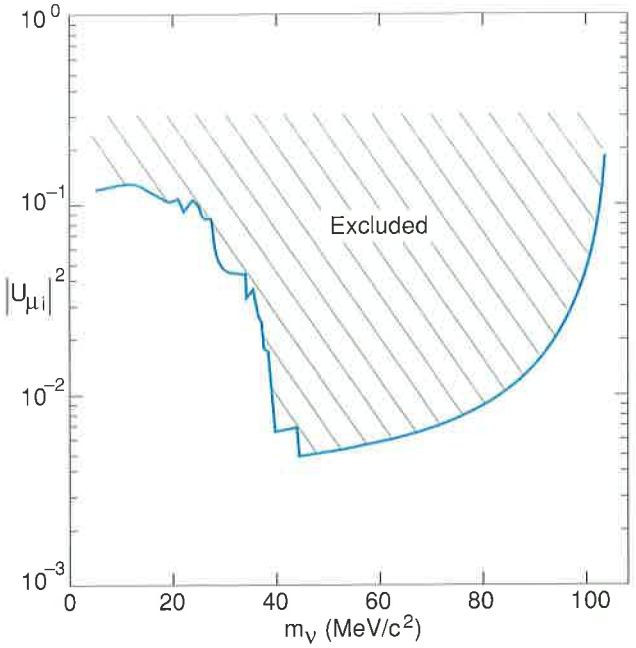

FIGURE 8

Maximum value of the mixing strength $|U_{\mu i}|^2$, deduced from the limited data discussed in this report, as a function of the neutrino mass.

References (Cont'd)

[3] R. Schrock, Phys. Lett. 96B (1980) 159;
R. Schrock, Phys. Rev. D24 (1891) 1232 and 1273.
[4] R. Abela et al., Phys. Lett. 105B (1981) 263.
[5] M. Daum et al., Phys. Rev. D36 (1987) 2624.
[6] R.S. Hayano et al., Phys. Rev. Lett. 49 (1982) 1305.
[7] Y. Asano et al., Phys. Lett. 104B (1981) 84.
[8] C.Y. Pang et al., Phys. Rev. D8 (1973) 1989.
[9] H. Albrecht et al., Phys. Lett. B202 (1988) 149.
[10] ALEPH Coll., D. Decamp et al., Phys. Lett. B231 (1989) 519;
ALEPH Coll., D. Decamp et al., Phys. Lett. B234 (1990) 209 and 399;
ALEPH Coll., D. Decamp et al., Phys. Lett. B236 (1990) 86 and 233;
DELPHI Coll., P. Aarnio et al., Phys. Lett. B231 (1989) 539;
L3 Coll., B. Adeva et al., Phys. Lett. B231 (1989) 509;
L3 Coll., B. Adeva et al., Phys. Lett. B233 (1989) 530;
L3 Coll., B. Adeva et al., Phys. Lett. B236 (1990) 109;
OPAL Coll., M.Z. Akrawy et al., Phys. Lett. B231 (1989) 530;
OPAL Coll., M.Z. Akrawy et al., Phys. Lett. B235 (1990) 379;
OPAL Coll., M.Z. Akrawy et al., Phys. Lett. B236 (1990) 364.
[11] J. Bernstein and G. Feinberg, Phys. Lett. B101 (1981) 39.
[12] J.P. Deutsch et al., Phys. Rev. D27 (1983) 1644.
[13] P.H. Frampton and P. Vogel, Phys. Reports 82 (1982) 339.
[14] J. Egger et al., proc. of the XVIth INS International Symposium, S. Kato and T. Ohshima eds, Inst. for Nucl. Study, Tokyo, World Scientific Publishing (1988) 266.
[15] J.A. Northrop and J. Gurski, Nucl. Instr. and Meth. 3 (1958) 207.
[16] D.R. Clay et al., Phys. Rev. B586 (1965) 140.
[17] B. Tasiaux, Thesis, UCL, to be published.

Addresses:

B. Tasiaux, A.S. Carnoy, J. Deutsch, S. Lontie, R. Prieels and N. Rosier
Institut de Physique Nucléaire
Université Catholique de Louvain
B–1348 Louvain-la-Neuve (Belgium)

J. Egger, H. Kaspar and C. Petitjean
Paul Scherrer Institute (PSI)
CH–5232 Villigen (Switzerland)

Received on 27 February 1991.